THE JOURNAL OF PHYSICAL CHEMISTRY LETTERS
A JOURNAL OF THE AMERICAN CHEMICAL SOCIETY

pubs.acs.org/JPCL Letter

Incorporating Solvation Effects in Oxidative Stability Predictions of Battery Electrolytes

John Holoubek,* Nicholas Solan, Zheng Chen, Ping Liu, and Tod A. Pascal*

Cite This: *J. Phys. Chem. Lett.* 2025, 16, 11398−11404 Read Online

ACCESS | Metrics & More | Article Recommendations | Supporting Information

ABSTRACT: Accurately predicting the oxidative stability of battery electrolytes is crucial for improving our understanding of high-voltage behavior and rational design of next-generation systems employing novel chemistries. However, commonly applied strategies based on evaluation of orbital occupancies of isolated molecules within density functional theory techniques neglect many-body solvation and interfacial effects that govern the electro-thermodynamics in real systems. Here, we advance a computational methodology that integrates molecular dynamics sampling of local solvation environments with explicit vertical ionization potential (IP) calculations to account for such effects. Our approach allows for both statistical accounting of IP distributions as well as prediction of the oxidized species (e.g., solvent vs anion decomposition). Application of this method to a matrix of electrolytes based on common lithium salts and solvents yields more detailed conclusions that often disagree with those gained through conventional calculations. We also demonstrate that this methodology can capture variations in IP associated with increased salt concentrations as well as the speciation and stability next to electrified model interfaces. This work offers a comprehensive accounting of the microscopic factors and electronic structure considerations that stabilize molecules and their unique solvation environment in modern electrochemical systems.

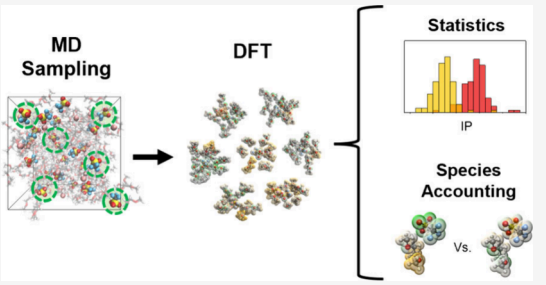

High-energy lithium batteries have become indispensable for modern portable electronics and electric transportation. While the energy density of these cells has slowly improved since their advent due to advances in cell engineering, we are approaching a maximum dictated by conventional electrode chemistries. One way to exceed this maximum is to increase the operating voltage of the cell, which can be done by implementing next-generation high-voltage cathodes,[1,2] or simply by increasing the operating voltage of conventional transition metal oxide cathodes (e.g., > 4.4 V vs Li).[3,4] Unfortunately, the cyclability of high-voltage systems is largely limited by parasitic decomposition of liquid electrolytes.[5,6]

Oxidative decomposition of the liquid electrolyte has largely been attributed to the thermodynamic stability of their chemical constituents, and the interfaces formed by their decomposition.[7−11] Accordingly, efforts to develop high voltage electrolytes commonly rely on the evaluation of the highest occupied (HOMO) and the lowest unoccupied (LUMO) molecular orbitals within density functional theory (DFT) of individual salt and solvent molecules to computationally predict and model the oxidative stability of electrolyte mixtures. These calculations frequently consider these species in vacuum or at simplified interfaces.[12−14] While these approaches provides a reasonable rapid screening methodology for system design, isolated DFT calculations, even more sophisticated ones that include screening by means of implicit solvent models, do not accurately consider the microscopic, intermolecular solvent interactions that are significant to the overall oxidation thermodynamics. Of note, *Kim et al.* demonstrated that the calculated ionization potential (IP) of solvent-anion pairs is significantly lower than isolated molecules or solvent−solvent pairs.[15] *Fadel et al.* later demonstrated that, applying exchange functionals that accurately capture discrete ionization behavior, this destabilization is a result of strong interactions between oxidized solvent species and anions.[16] We denote these calculations as pair-DFT forthwith.

While pair-DFT calculations often offer greater accuracy in predicting oxidative stability compared to those of isolated species, there are also clear limitations associated with this approach. Critically, they cannot capture the many body interactions present in real liquid electrolytes, since these calculations commonly rely on geometry optimization protocols that yield a single, lowest energy configuration. In other words, they lack the ability to average over ensemble structures, each with finite occurrence probabilities (i.e., entropic effects) and varying binding energies (enthalpic

Received: September 24, 2025
Revised: October 21, 2025
Accepted: October 23, 2025
Published: October 24, 2025

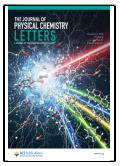

https://doi.org/10.1021/acs.jpclett.5c02984
J. Phys. Chem. Lett. 2025, 16, 11398−11404

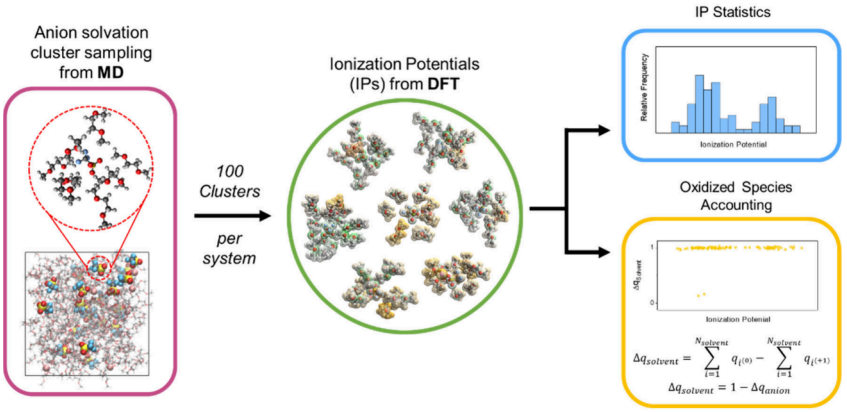

Figure 1. Schematic description of the IP sampling method, consisting of anion-centered cluster sampling from MD, ionization potential calculation from DFT, and statistical accounting.

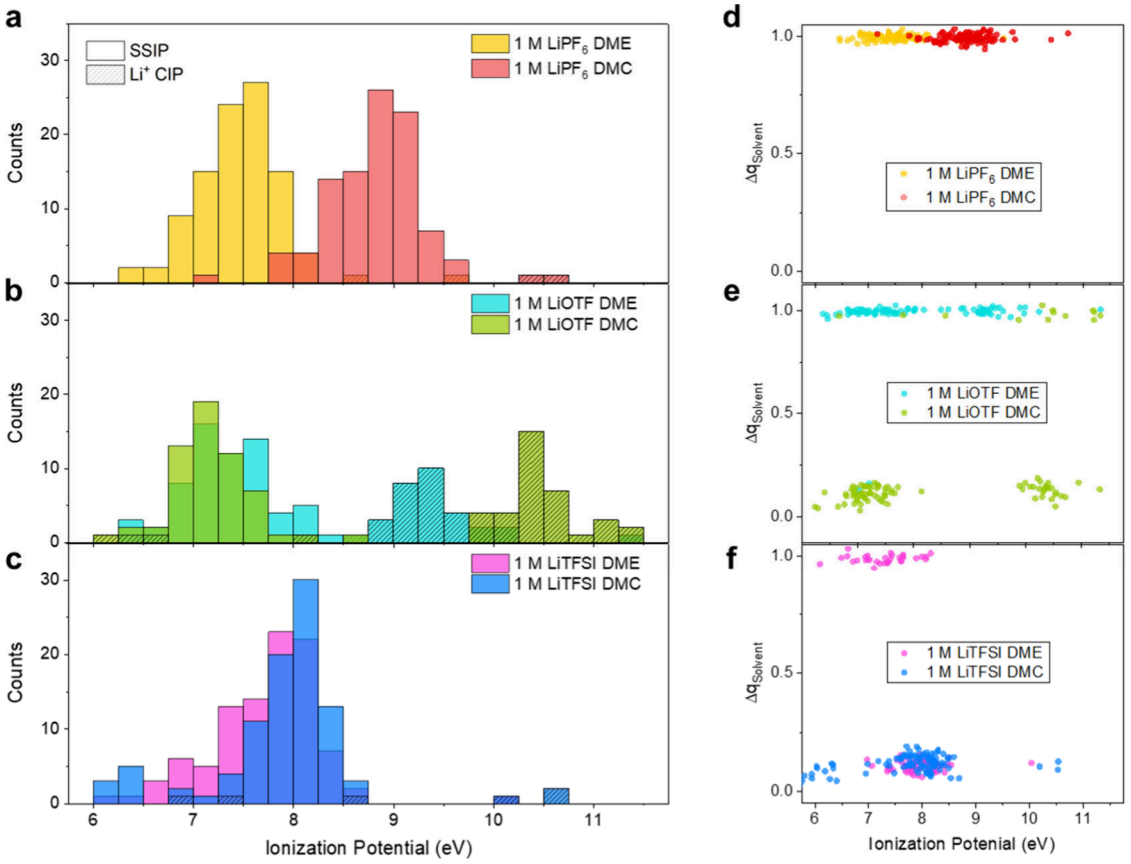

Figure 2. Ionization potential distributions generated from sampling of **a)** 1 M $LiPF_6$, **b)** 1 M LiOTF, and **c)** 1 M LiTFSI systems. Ionized species accounting from **d)** 1 M $LiPF_6$, **e)** 1 M LiOTF, and **f)** 1 M LiTFSI system sampling.

effects), that rigorously defines the solvation free energy landscape for the ions. Moreover, these ensemble structures, which are sometimes additionally classified into unique families based on local coordination environments, can have variable IPs.[16−18] Given this limitation, it is therefore not surprising that isolated or pair-DFT would not be able to accurately describe the well-known experimental dependence of oxidative stability on the concentration of salt in the electrolyte.[19−21] Additionally, they cannot predict the species in a given cluster that is most likely to undergo oxidation, a critical factor for determining the composition of the cathode-electrolyte-interphase (CEI), which is also likely dependent on atomic configuration.[8]

In this work, we develop a computational methodology to incorporate the effects of solvation structure and electrolyte composition into oxidative stability predictions (Figure 1). We sample local molecular clusters from classical molecular dynamics (MD) simulations of electrolytes of interest, which produce statistically converged ensembles that define the thermodynamic solvation states, relevant to oxidative stability. These molecular clusters are subjected to IP calculations in DFT *without geometry optimization* to obtain a distribution of IPs for the electrolyte in question. Employing explicit

https://doi.org/10.1021/acs.jpclett.5c02984
J. Phys. Chem. Lett. 2025, 16, 11398−11404

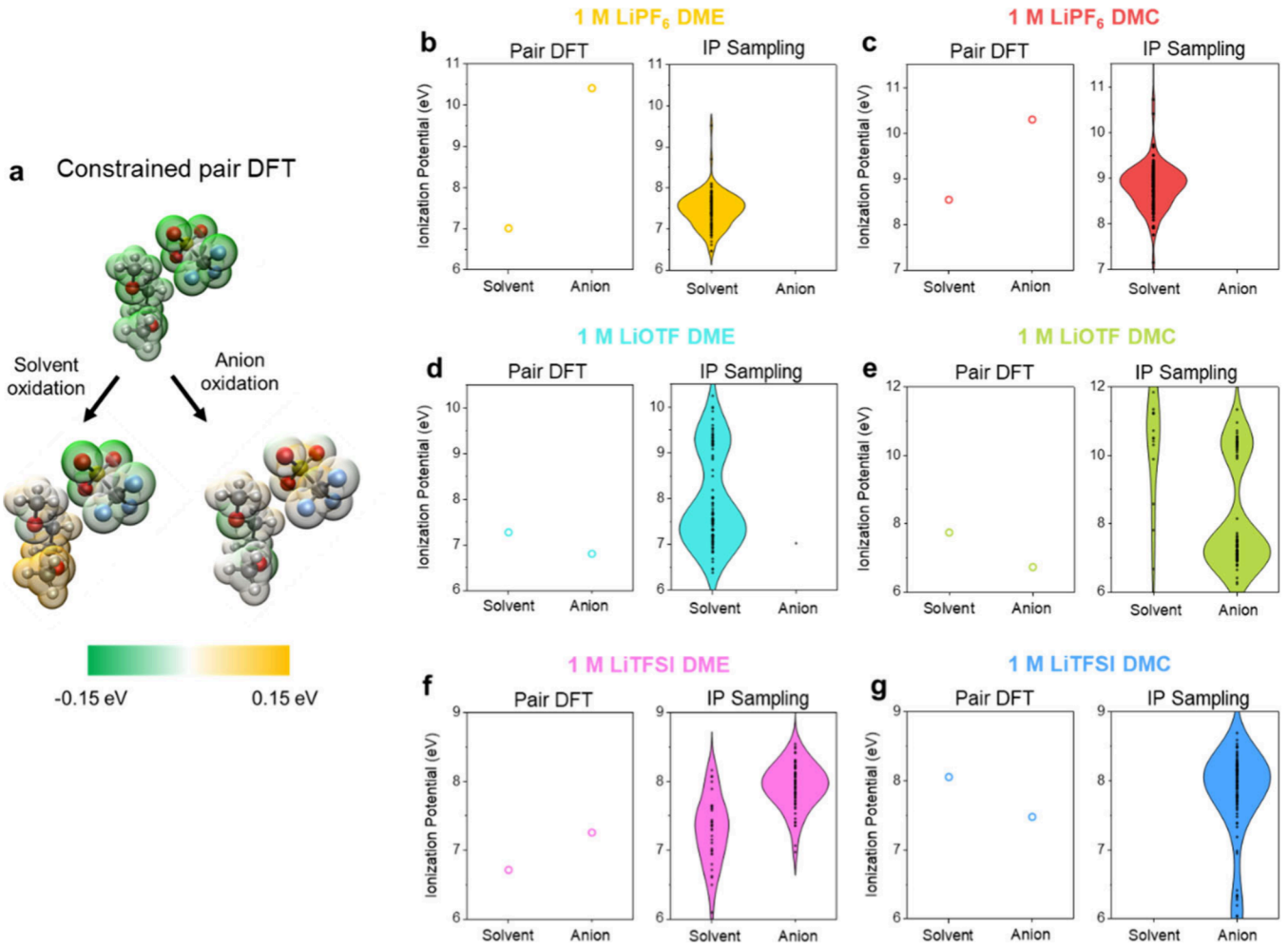

Figure 3. Comparison of oxidation behavior predictions from anion/solvent pair DFT and IP Sampling. **a)** Electrostatic potential maps of anion/solvent pairs before and after solvent or anion oxidation. The OTF^-/DME pair is shown as a representative example. Anion and solvent ionization energies from constrained pair DFT and solvent/anion IP distributions in **b)** 1 M $LiPF_6$ DME, **c)** 1 M $LiPF_6$ DMC, **d)** 1 LiOTF DME, **e)** 1 M LiOTF DMC, **f)** 1 M LiTFSI DME, and **g)** 1 M LiTFSI DMC.

ionization calculations with properly selected exchange functionals[16] further enables the determination of oxidized species (in this case, solvent vs anion) via the accounting of atomic partial charge. Our approach offers a means to directly predict the states that define the ionization potential of well-defined electrolyte compositions and gain insights into their oxidative decomposition route. We demonstrate this in a variety of electrolyte chemistries and salt concentrations, comparing our predictions to that of conventional pair-DFT, and show how it can be extended toward simulating model electrochemical interfaces.

Before conducting IP sampling on model electrolytes, we first benchmark our approach using model solutions of lithium trifluoromethanesulfonate (LiOTF) in 1,2-dimethoxyethane (DME). Previous works have demonstrated that the least oxidatively stable configurations of the electrolyte originate from the local structures surrounding the anion.[16] Indeed, the IP distribution of clusters surrounding the anions are significantly lower than those solvating the cations, due to stabilizing effect of electron donation to Li^+ (Figure S1). We therefore conduct sampling of solvation clusters from the MD trajectories centered on the anions present in solution, conducted based on a sampling cutoff defined as the atom-to-atom distance between any atoms in the anion and surrounding molecules. For DFT-based IP calculations on the sampled clusters, we apply the M06-HF exchange functional, which was previously shown to produce accurate, discrete ionization behavior.[16,22] We also find that a 3 Å sampling cutoff produces similar IP distributions to 3.5 Å at a significantly reduced system size, and that the 6−31+G* basis set produces similar accuracy to the 6−311++G** set (Figures S2, S3). Hence, we adopt an anion-centered sampling methodology with a 3 Å cutoff and IP calculations at the M06-HF//6−31+G* level of theory. To strike a balance between statistical robustness and computational cost, we sample 100 snapshots around 25 random anions in the MD trajectory temporally spaced evenly across the last 5 ns of production dynamics, corresponding to a sampling stride of 1.25 ns.

We next apply this sampling methodology to 1 M solutions of lithium hexafluorophosphate ($LiPF_6$), lithium bis(trifluoro sulfonyl)imide (LiTFSI), and LiOTF in DME and dimethyl carbonate (DMC). This system matrix, where carbonate solvents are more oxidatively stable than ethers, and known anion oxidative stability is in order of OTF^- < $TFSI^-$ < PF_6^- (Figure S4) provides a rigorous test of our approach. Among the 6 systems, we find that the largest variance in solvation behavior occurs as a function of anion identity, where $LiPF_6$

https://doi.org/10.1021/acs.jpclett.5c02984
J. Phys. Chem. Lett. 2025, 16, 11398−11404

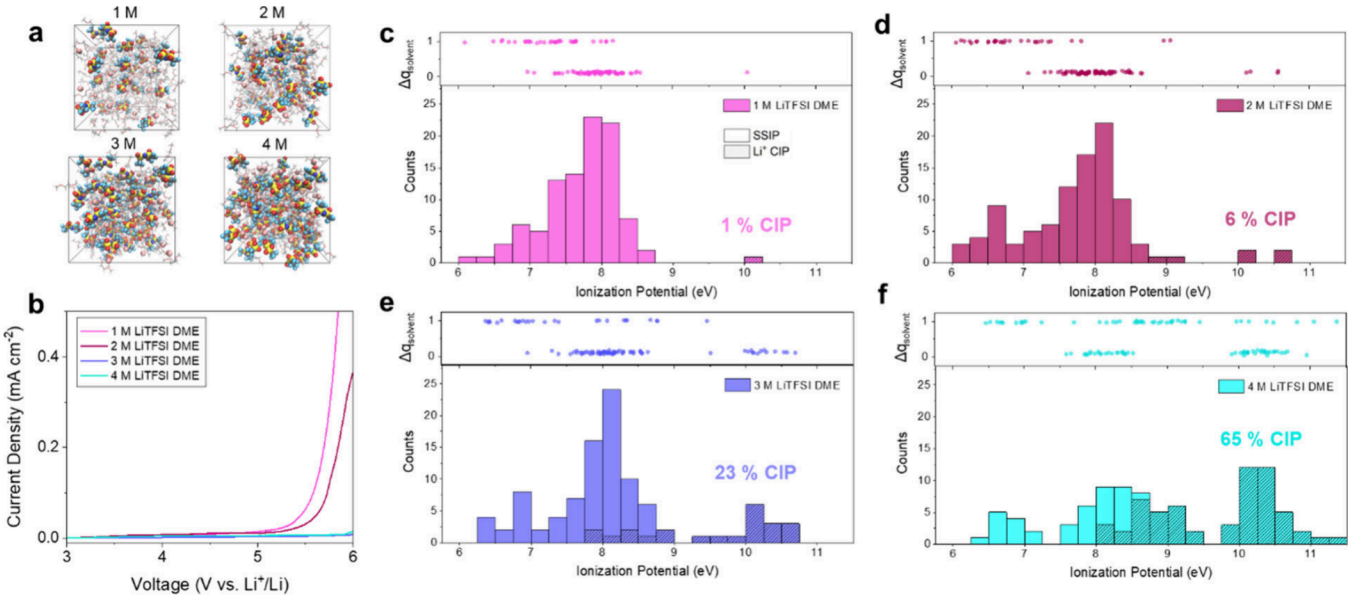

Figure 4. Effect of electrolyte concentration on ionization potential distributions. **a**) Snapshots of MD simulations of 1−4 M LiTFSI DME. **b**) Linear scan voltammetry of Li//Al coin cells containing 1−4 M LiTFSI DME. Ionization potential distributions and ionized species accounting of **c**) 1 M, **d**) 2 M, **e**) 3 M, and **f**) 4 M LiTFSI DME systems.

tends to produce the least amount of ion pairing (Figures S5, S6). We also find that at 1 M, the LiOTF system displays ion-pairing with a single anion per Li^+, referred to as a contact-ion-pair (CIP). All 1 M systems are otherwise dominated by solvent-separated-ion-pairs (SSIPs).

As shown in Figure 2, the resulting IP distributions are multimodal and normal, with individual peaks attributable to structures that do and do not contain a Li^+ ion. In general, we find that Li^+ coordination stabilizes the HOMO of solvating species, in agreement with a previous work.[23] For 1 M $LiPF_6$ systems, our calculations indicate that the solvents would be oxidized and decompose first, due to the extreme stability of PF_6, where the DMC system is ∼ 1 eV more stable due to the solvent's inherent stability (Figure 2a,d). In 1 M LiOTF and 1 M LiTFSI systems, where anion and solvent decomposition are found at similar levels, the predicted oxidative behavior is less straightforward. Of note, the presence of anion vs solvent decomposition can be completely different, despite ostensibly similar distributions for the least stable clusters (Figure 2b,c,e,f).

To judge the relative utility of our IP sampling method, we then compare to the predictions of conventional pair-DFT calculations.[15,16] Using fragmentation-based constrained DFT, we also assess the IP for explicit ionization of either the anion or solvent within each pair (Figure 3a). We find that agreement between the decomposition energies from the two methods are highly system dependent. First, both approaches tend to agree in both the energetics and the identity of the decomposed species for the 1 M $LiPF_6$ electrolytes, which is intuitive given the large discrepancy between the inherent IP of PF_6^- and solvents (Figure 3b,c). However, for systems in which the anion and solvent IP are similar, significant discrepancies between pair-DFT and IP sampling are observed. In the 1 M LiOTF DME system, we find that the IP sampling predictions directly contradict the pair DFT predictions, where the IP distribution is dominated by solvent decomposition despite more favorable anion decomposition in the pair (Figure 3d). The 1 M LiOTF DMC IP distribution, by comparison, is closer to the pair-DFT predictions, again likely due to the disparate IPs of DMC and OTF^- (Figure 3e). In 1 M LiTFSI DME, the solvent is also predicted to be less stable by ∼ 0.5 eV, even though the solvent molecules represent a relatively small portion of the predicted decomposition species from IP sampling (Figure 3f). In these systems, in which the isolated anion and solvent IPs are somewhat competitive with one another as defined by a solvent IP shift of −2.8 eV by Fadel et al., the effects of local configuration and many-body effects meaningfully shift the predicted decomposition species.[16] In the case of 1 M LiTFSI DME, for example, the prediction of both anion and solvent decomposition agrees with our previous experimental work that observed both organic and salt-derived CEI species, which would not be predicted by pair-DFT alone.[24]

As previously mentioned, current IP prediction methods cannot capture the effect of salt concentration on the electrolyte's oxidative stability, where a higher ratio of salt:solvent results in a higher prevalence of ion-pairing, stabilizing the anion and surrounding solvent toward oxidation. To test this hypothesis, we considered DME systems of LiTFSI concentration ranging from 1 to 4 M (Figure 4a). Experimentally we find an increase in oxidative breakdown voltage with increasing concentration (Figure 4b). Indeed, the calculated IP distributions from these systems do show a steady depopulation of the least stable IP state which are composed of clusters that are not Li^+ coordinated (Figure 4c-f). Similarly, we find an increase in highly stable Li^+ coordinated clusters. Interestingly, the persistence of some low IP solvation states (which are primarily SSIP) would not describe the experimentally observed monotonic increase in decomposition onset if interpreted with a standard Boltzmann probability analysis. This warrants greater attention and will be the subject of follow-up work.

So far, we have argued that conducting IP predictions from sampled clusters from MD simulations of bulk electrolytes is more accurate and describes more phenomena than conventional DFT methods. However, this method still inherently

https://doi.org/10.1021/acs.jpclett.5c02984
J. Phys. Chem. Lett. 2025, 16, 11398−11404

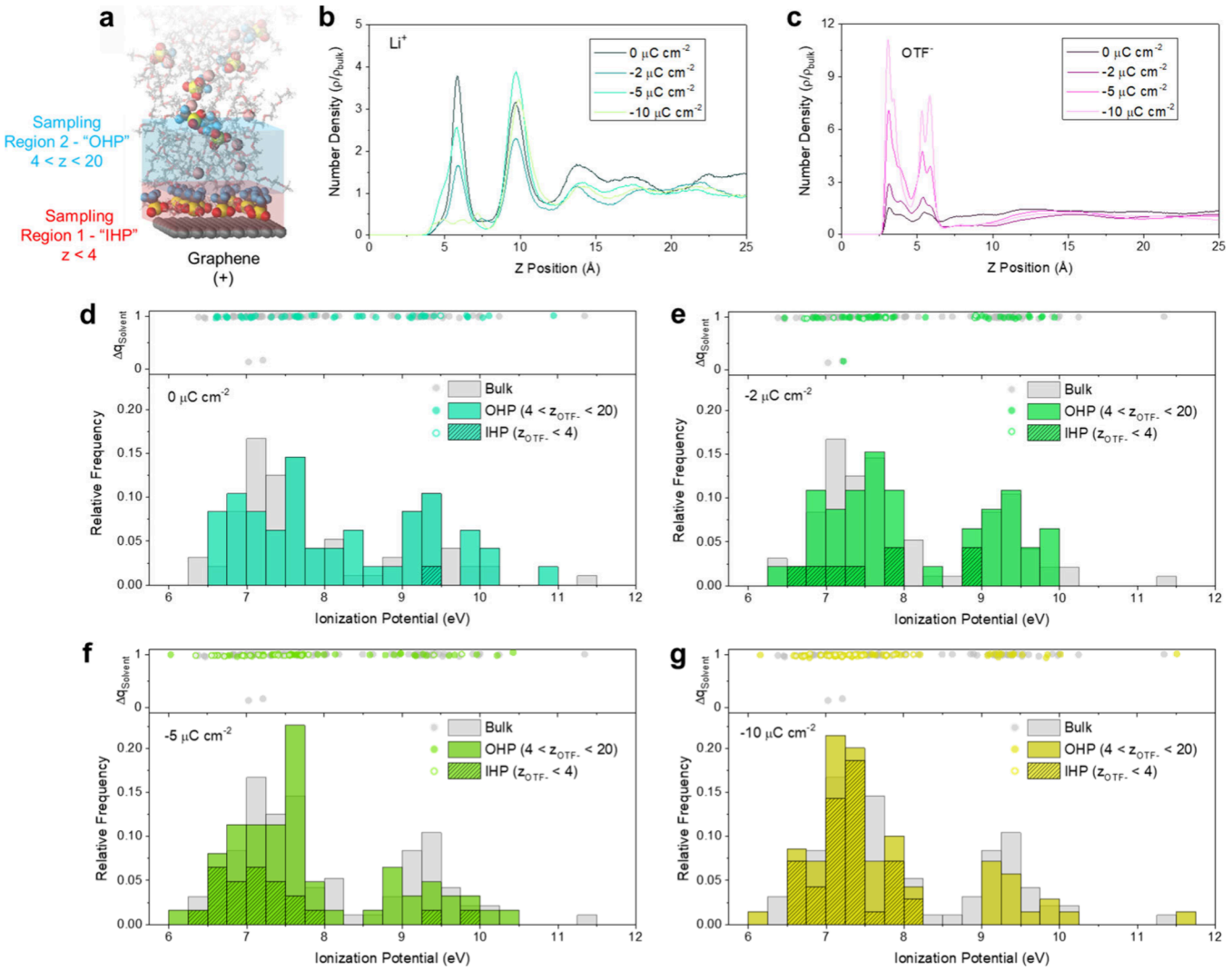

Figure 5. Ionization potential sampling at model electrode/electrolyte interfaces. **a**) Representative visualization of a graphene/1 M LiOTF MD cell at −10 μC cm^{-2} with highlighted sampling regions. Number density profiles of **b**) Li^+ and **c**) OTF^- as a function of electrode bias. Ionization potential distributions and ionized species accounting for 1 M LiOTF DME at graphene at **d**) 0, **e**) −2, **f**) −5, and **g**) −10 μC cm^{-2}.

assumes that bulk solvation structures are representative of the local environment of electrochemical interfaces, where oxidative decomposition actually occurs. To demonstrate that this IP sampling method can in fact capture interfacial effects, we apply it to MD simulations at model graphene/electrolyte systems at between 0 and −10 μC cm^{-2} (Supporting Information, Figure S7). Although the relationship between surface charge density and electrode potential is difficult to estimate, we believe these conditions are somewhat representative of cathode operating conditions given a double layer capacitance of 10s of μF cm^{-2} and a potential of zero charge near 3 V vs Li/Li$^+$.[25] 1 M LiOTF DME was selected due to the presence of ion pairs at 1 M concentration. For the purposes of the sampling done in this work, we simplify the regions of interest in these interfacial simulations as the following: 1) The inner Helmholtz plane (IHP), defined by species in direct contact with the electrode (distance <4 Å), and 2) The outer Helmholtz plane (OHP), 4 < distance < 20 Å (Figure 5a). We compare the IP distributions sampled from these regions with the bulk distributions obtained previously. The electrode near which sampling is conducted is sequentially charged in the (+) direction (corresponding to negative interfacial charge) to understand the impact of bias on the IP distributions within the EDL. It is also critical to note that any direct binding interactions and the corresponding renormalization of the electronic structures between the interface and the electrolyte are not considered via this methodology, and would need to be considered by a coupled simulation that also considers quantum mechanics, such as those developed by *Shin et al.*[26]

As shown in Figure 5b,c, the introduction of a positive bias on the graphene electrode results in a depletion of Li^+ and enrichment of OTF^- at the interface due to electrostatic repulsion and attraction, respectively. Comparatively, this bias has little influence on the presence of neutral solvent molecules (Figures S7, S8). Moreover, although there is minimal anion adsorption at 0 and −2 μC cm^{-2}, the IP distributions of clusters from the OHP, which contain directly adsorbed solvents, are relatively similar to bulk systems (Figure 5d,e). However, at increased surface bias, anions in the IHP begin to have a more pronounced influence in the overall IP distribution (Figure 5f,g). Critically, under these conditions, the repulsion of Li^+ from the interface induces a depopulation of highly stable CIP clusters from the IHP, indicating a destabilizing effect of positive electrode charge. Although

https://doi.org/10.1021/acs.jpclett.5c02984
J. Phys. Chem. Lett. 2025, 16, 11398−11404

adjustments to the protocol should be made to more accurately sample the states that dictate electrolyte oxidation at the interface, these results suggest a reasonable ability of bulk IP sampling to capture more complicated interfacial phenomena.

In this work, we introduce a statistical IP sampling methodology that integrates MD and DFT to more accurately predict the oxidative stability of lithium battery electrolytes. Unlike traditional pair-DFT approaches, which are limited by finite size and minimum energy structure effects, this method captures the distribution of oxidation potentials across molecular clusters whose composition and internal orientation are thermodynamically converged from larger-scale classical MD. Applied to a range of salt−solvent combinations and concentrations, the approach reveals that oxidative stability is highly sensitive to Li^+-anion interactions. We also find that the identity of the oxidized species can differ substantially from pair-DFT approaches, particularly for systems in which the anion and solvent are similar in inherent stability. This method reproduces the well-known experimental correlation between oxidative stability and salt concentration and is capable of capturing shifts in IP distributions under applied electrostatic bias at model electrode/electrolyte interfaces. This approach advances a more sophisticated and nuanced view solvation in battery electrolytes, which can be easily applied to more generally to understanding oxidative and reductive stability of electrolytes in energy storage systems.

■ ASSOCIATED CONTENT

Supporting Information

The Supporting Information is available free of charge at https://pubs.acs.org/doi/10.1021/acs.jpclett.5c02984.

Detailed computational methods, MD simulation parameters, effect of cluster sampling species, cutoff, and DFT basis set, isolated ionization potentials, radial distribution functions from MD, interfacial MD renderings, density profiles, and charge densities (PDF)

■ AUTHOR INFORMATION

Corresponding Authors

John Holoubek − *Department of Materials Science and Engineering, Stanford University, Stanford, California 94305, United States; Aiiso Yufeng Li Family Department of Chemical and Nano Engineering, University of California San Diego, La Jolla, California 92093, United States;* orcid.org/0000-0003-0015-4512; Email: jholo@stanford.edu

Tod A. Pascal − *Aiiso Yufeng Li Family Department of Chemical and Nano Engineering, Program of Materials Science and Engineering, and Sustainable Power and Energy Center, University of California San Diego, La Jolla, California 92093, United States;* orcid.org/0000-0003-2096-1143; Email: tpascal@ucsd.edu

Authors

Nicholas Solan − *Aiiso Yufeng Li Family Department of Chemical and Nano Engineering, University of California San Diego, La Jolla, California 92093, United States;* orcid.org/0009-0007-8884-4249

Zheng Chen − *Aiiso Yufeng Li Family Department of Chemical and Nano Engineering, Program of Materials Science and Engineering, and Sustainable Power and Energy Center, University of California San Diego, La Jolla, California 92093, United States;* orcid.org/0000-0002-9186-4298

Ping Liu − *Aiiso Yufeng Li Family Department of Chemical and Nano Engineering, Program of Materials Science and Engineering, and Sustainable Power and Energy Center, University of California San Diego, La Jolla, California 92093, United States;* orcid.org/0000-0002-1488-1668

Complete contact information is available at: https://pubs.acs.org/10.1021/acs.jpclett.5c02984

Author Contributions

J.H. conceived the original idea. Z.C., P.L., and T.A.P. directed the project. J.H. developed the scripts and conducted the simulations under the guidance of T.A.P. N.S. conducted the experiments. J.H. wrote the manuscript. All authors discussed the results and edited the manuscript.

Notes

The authors declare no competing financial interest.

■ ACKNOWLEDGMENTS

This work was supported by NASA Space Technology Graduate Research Opportunity 80NSSC20K1174. This work was partially supported by the US National Science Foundation grant CBET-309147 (N.S.). Portions of this work were supported by the US Department of Energy EERE VTO program, through grant DE-SC0023503. Part of the work used the UCSD-MTI Battery Fabrication Facility and the UCSD-Arbin Battery Testing Facility. This work used the Expanse supercomputer at the San Diego Supercomputing center through allocation PHY200077 from the Advanced Cyberinfrastructure Coordination Ecosystem: Services & Support (ACCESS) program, which is supported by National Science Foundation grants #2138259, #2138286, #2138307, #2137603, and #2138296.

■ REFERENCES

(1) Li, W.; Song, B.; Manthiram, A. High-Voltage Positive Electrode Materials for Lithium-Ion Batteries. *Chem. Soc. Rev.* **2017**, *46* (10), 3006−3059.

(2) Xiang, J.; Wei, Y.; Zhong, Y.; Yang, Y.; Cheng, H.; Yuan, L.; Xu, H.; Huang, Y. Building Practical High-Voltage Cathode Materials for Lithium-Ion Batteries. *Adv. Mater.* **2022**, *34* (52), No. 2200912.

(3) Zhang, L.; Zhang, C.; Li, N.; Tong, W. Influence of Charge Cutoff Voltage on the Cycling Behavior of LiNi0.5Mn0.3Co0.2O2 Cathode. *J. Electrochem. Soc.* **2020**, *167* (12), No. 120509.

(4) Wu, Q.; Zhang, B.; Lu, Y. Progress and Perspective of High-Voltage Lithium Cobalt Oxide in Lithium-Ion Batteries. *Journal of Energy Chemistry* **2022**, *74*, 283−308.

(5) Choi, N.-S.; Han, J.-G.; Ha, S.-Y.; Park, I.; Back, C.-K. Recent Advances in the Electrolytes for Interfacial Stability of High-Voltage Cathodes in Lithium-Ion Batteries. *RSC Adv.* **2015**, *5* (4), 2732−2748.

(6) Fan, X.; Wang, C. High-Voltage Liquid Electrolytes for Li Batteries: Progress and Perspectives. *Chem. Soc. Rev.* **2021**, *50* (18), 10486−10566.

(7) Zhang, Z.; Hu, L.; Wu, H.; Weng, W.; Koh, M.; Redfern, P. C.; Curtiss, L. A.; Amine, K. Fluorinated Electrolytes for 5 V Lithium-Ion Battery Chemistry. *Energy Environ. Sci.* **2013**, *6* (6), 1806−1810.

(8) Fan, X.; Chen, L.; Ji, X.; Deng, T.; Hou, S.; Chen, J.; Zheng, J.; Wang, F.; Jiang, J.; Xu, K.; Wang, C. Highly Fluorinated Interphases Enable High-Voltage Li-Metal Batteries. *Chem.* **2018**, *4* (1), 174−185.

(9) Cao, X.; Jia, H.; Xu, W.; Zhang, J.-G. Review—Localized High-Concentration Electrolytes for Lithium Batteries. *J. Electrochem. Soc.* **2021**, *168* (1), No. 010522.
(10) Fan, X.; Chen, L.; Borodin, O.; Ji, X.; Chen, J.; Hou, S.; Deng, T.; Zheng, J.; Yang, C.; Liou, S.-C.; Amine, K.; Xu, K.; Wang, C. Non-Flammable Electrolyte Enables Li-Metal Batteries with Aggressive Cathode Chemistries. *Nat. Nanotechnol.* **2018**, *13* (8), 715−722.
(11) Wei, Z.; Yuan, D.; Yuan, X.; Zhang, Y.; Ma, J.; Zhang, S.; Zhang, H. Formulation Principles and Synergistic Effects of High-Voltage Electrolytes. *Chem. Soc. Rev.* **2025**, *54* (8), 3775−3818.
(12) Han, J.-G.; Lee, J. B.; Cha, A.; Lee, T. K.; Cho, W.; Chae, S.; Kang, S. J.; Kwak, S. K.; Cho, J.; Hong, S. Y.; Choi, N.-S. Unsymmetrical Fluorinated Malonatoborate as an Amphoteric Additive for High-Energy-Density Lithium-Ion Batteries. *Energy Environ. Sci.* **2018**, *11* (6), 1552−1562.
(13) Borodin, O. Challenges with Prediction of Battery Electrolyte Electrochemical Stability Window and Guiding the Electrode − Electrolyte Stabilization. *Current Opinion in Electrochemistry* **2019**, *13*, 86−93.
(14) Leung, K. First-Principles Examination of Multiple Criteria of Organic Solvent Oxidative Stability in Batteries. *Chem. Mater.* **2023**, *35* (6), 2518−2530.
(15) Kim, D. Y.; Park, M. S.; Lim, Y.; Kang, Y.-S.; Park, J.-H.; Doo, S.-G. Computational Comparison of Oxidation Stability: Solvent/Salt Monomers vs Solvent−Solvent/Salt Pairs. *J. Power Sources* **2015**, *288*, 393−400.
(16) Fadel, E. R.; Faglioni, F.; Samsonidze, G.; Molinari, N.; Merinov, B. V.; Goddard, W. A., III; Grossman, J. C.; Mailoa, J. P.; Kozinsky, B. Role of Solvent-Anion Charge Transfer in Oxidative Degradation of Battery Electrolytes. *Nat. Commun.* **2019**, *10* (1), 1−10.
(17) Baskin, A.; Prendergast, D. "Ion Solvation Spectra": Free Energy Analysis of Solvation Structures of Multivalent Cations in Aprotic Solvents. *J. Phys. Chem. Lett.* **2019**, *10* (17), 4920−4928.
(18) Roncoroni, F.; Sanz-Matias, A.; Sundararaman, S.; Prendergast, D. Unsupervised Learning of Representative Local Atomic Arrangements in Molecular Dynamics Data. *Phys. Chem. Chem. Phys.* **2023**, *25* (19), 13741−13754.
(19) Yoshida, K.; Nakamura, M.; Kazue, Y.; Tachikawa, N.; Tsuzuki, S.; Seki, S.; Dokko, K.; Watanabe, M. Oxidative-Stability Enhancement and Charge Transport Mechanism in Glyme−Lithium Salt Equimolar Complexes. *J. Am. Chem. Soc.* **2011**, *133* (33), 13121−13129.
(20) Ren, X.; Zou, L.; Jiao, S.; Mei, D.; Engelhard, M. H.; Li, Q.; Lee, H.; Niu, C.; Adams, B. D.; Wang, C.; Liu, J.; Zhang, J.-G.; Xu, W. High-Concentration Ether Electrolytes for Stable High-Voltage Lithium Metal Batteries. *ACS Energy Lett.* **2019**, *4* (4), 896−902.
(21) Yamada, Y.; Yamada, A. Review—Superconcentrated Electrolytes for Lithium Batteries. *J. Electrochem. Soc.* **2015**, *162* (14), A2406−A2423.
(22) Zhao, Y.; Truhlar, D. G. The M06 Suite of Density Functionals for Main Group Thermochemistry, Thermochemical Kinetics, Noncovalent Interactions, Excited States, and Transition Elements: Two New Functionals and Systematic Testing of Four M06-Class Functionals and 12 Other Functionals. *Theor. Chem. Acc.* **2008**, *120* (1), 215−241.
(23) Pande, V.; Viswanathan, V. Descriptors for Electrolyte-Renormalized Oxidative Stability of Solvents in Lithium-Ion Batteries. *J. Phys. Chem. Lett.* **2019**, *10* (22), 7031−7036.
(24) Holoubek, J.; Yan, Q.; Liu, H.; Hopkins, E. J.; Wu, Z.; Yu, S.; Luo, J.; Pascal, T. A.; Chen, Z.; Liu, P. Oxidative Stabilization of Dilute Ether Electrolytes via Anion Modification. *ACS Energy Lett.* **2022**, *7*, 675−682.
(25) Zebardast, H. R.; Rogak, S.; Asselin, E. Potential of Zero Charge of Glassy Carbon at Elevated Temperatures. *J. Electroanal. Chem.* **2014**, *724*, 36−42.
(26) Shin, S.-J.; Choi, H.; Ringe, S.; Won, D. H.; Oh, H.-S.; Kim, D. H.; Lee, T.; Nam, D.-H.; Kim, H.; Choi, C. H. A Unifying Mechanism for Cation Effect Modulating C1 and C2 Productions from CO2 Electroreduction. *Nat. Commun.* **2022**, *13* (1), 5482.

https://doi.org/10.1021/acs.jpclett.5c02984
J. Phys. Chem. Lett. 2025, 16, 11398−11404